

Capacity, Coverage and Power Profile Performance Evaluation of a Novel Rural Broadband Services Exploiting TVWS From High Altitude Platform

HABIB MOHAMMED HUSSEIN ¹, KONSTANTINOS KATZIS ² (Senior Member, IEEE),
LUZANGO PANGANI MFUPE ³ (Senior Member, IEEE),
AND EPHREM TESHALE BEKELE ¹ (Senior Member, IEEE)

¹Department of Electrical and Computer Engineering, Addis Ababa Institute of Technology, Addis Ababa 1000, Ethiopia

²European University of Cyprus, 2404 Nicosia, Cyprus

³CSIR, Brummeria, Pretoria 0184, South Africa

CORRESPONDING AUTHOR: HABIB MOHAMMED HUSSEIN (e-mail: habib.mohammed@aait.edu.et)

ABSTRACT The coverage and capacity of exploiting TV White Spaces (TVWS) from High Altitude Platforms (HAPs) with multiple antenna payloads using uniform rectangular phased array (URA) antennas are explored in this article. A scenario is suggested in which a HAP and TVWS base station are installed on the HAP within a HAP coverage area with a radius of 100 km and a cell radius of 10.5 km. The formation of HAP cells with various reuse patterns has been established. An analysis of coverage, capacity and power profile function for TVWS link from 25×25 URA HAP arrays is presented. To minimize the sidelobe levels in the antenna array synthesis, window function has been assumed. Power profile within a cell using URA is highlighted. Channel to Interference (CIR) performance contour, coverage probability and channel capacity have been determined. The channel capacity for the theoretical Shannon bound and practical truncated Shannon bound are determined and compared. Results show that a maximum channel capacity of 53 Mbps can be attained from the proposed model.

INDEX TERMS Array antenna, array factor, beamwidth, capacity, CINR, CIR, high altitude platform, power profile, sidelobe level, TVWS.

I. INTRODUCTION

Internet access has changed numerous aspects of our lives by offering far-reaching economic and social benefits. Because of this, a plethora of newly featured wireless gadgets are increasingly growing, needing considerable radio spectrum for their operation. It has to be effectively managed as wireless spectrum is a naturally scarce resource. In the years 2018 to 2020, CISCO virtual network index forecasts that by 2023, there will be 29.3 billion networked devices [1]. Additional capacity is appropriate for such growth. This can be done by allocating additional spectrum in congested areas or by adding small-size cells. Despite this dramatic increase in internet use,

almost half of the world's population is still unconnected [2]. Sixty percent to seventy percent of the world lives in developing countries [3].

As per the study in [4], a 10% rise in broadband coverage will also increase the global growth rate by 1.38%. For example, 80% of Ethiopia's population resides in rural regions. Providing internet access to rural areas would serve much of the nation's needs efficiently, thus boosting the country's economic growth. In sparsely inhabited environments, the introduction of traditional communication networks by telecom operators is not economically feasible. Researchers around the world are actively investigating the prospect of utilizing the

underused/unused part of the TV spectrum (more specifically for the UHF band) known as TV White Space (TVWS) as a low-cost solution to wireless broadband network [4], [5], [6]. The deployment of TVWS networks from High Altitude Platforms (HAPs) using UHF bands is an effective way of delivering wireless broadband connectivity to such areas [7]. HAPs are airships or aircraft operating in the stratosphere around 17–22 km above ground [8], [9]. They are carrying a number of wireless transceivers collocated on the platform, which have the capability of handling a large number of users. This is achieved due to the fact that the aerial platform offers Line-of-Sight (LoS) communications to a vast geographical coverage area. The architecture of HAPs allows them to utilize frequencies that may be problematic for other networks to utilize [10]. Using HAPs to deliver telecommunications services is a financially viable alternative, according to the research in [4], [11] and [12]. The authors emphasized that the common benefits of broadband penetration in rural nations include improved education and health service delivery, community development and small business expansion, prevention of rural-urban migration, and interaction between communication infrastructure and various services. The literature in [11] and [12] demonstrated the advantages of HAPs over terrestrial wireless and satellite systems in handling certain wireless communication challenges. The cost advantages of HAPs over terrestrial systems are sufficiently reflected in the assessments.

According to [11], the cost of deploying, running, and maintaining a 1 km radius macrocell is around 168 thousand euros (9.744 million birr). At least 900 such macrocells are required to provide continuous coverage within a 30 km radius. As a consequence, the network's estimated cost is 151 million euros (8.758 billion birr), which is rather high. According to [24], the expected cost of deploying, operating, and maintaining a HAP is around 5 million euros (290 million birr) for unmanned solar aircraft to serve the same service territory. HAPs give higher coverage at a reduced cost, are simple to install, and can be used for a prolonged period of time [11]. These advantages meet the criteria for a rural wireless communication system, demonstrating that HAPs are a feasible alternative for rural wireless communication. Previous studies indicated that HAPs were allocated frequency bands requiring LoS communication suffering from severe rain attenuation [14]. However, HAPs may be used to allow use of a large variety of bands. More precisely, HAP devices have been given the following spectrum by the ITU: 47.2–47.5 GHz, 47.9–48.2 GHz, 38–39.6 GHz, 31.3 GHz, 27.9–28.2 GHz, 24.25–27.5 GHz, 21.4–22 GHz (Region 2) and 6440–6520 MHz, 6560–6640 MHz [15]. As has been shown by several works, certain communication systems such as HAPs may use their abilities to deliver certain services that conventional systems such as terrestrial systems deliver [9], [16]–[18]. When considering the convergence of HAP with other legacy networks, like WIMAX and WIFI, many references may be found in the literature [19]–[22]. Furthermore, the work presented in [23] and [24] discusses HAPs extended coverage with dispersed and hotspot

users, multi-input multi-output (MIMO) and beamforming techniques. Results show how cell edge HAP beams have diminished links and significantly increased side lobe quantities have dominated due to co-channel interference. In [25], an antenna array approach was presented for high data-rate transmission by using HAPs for trains. Project Loon included the idea of using high-altitude balloons to deliver internet access and coverage to unserved and underserved regions [26]. Authors in [27] have also highlighted the capability of Long-Term Evolution (LTE) from HAP utilizing 700 MHz Spectrum. The study in [28], presented the idea of providing wireless TVWS broadband from a meshed network of HAPs and terrestrial base stations. This work did not however conduct a numerical study and estimation of the proposed method. The work in [4], introduced a novel type of architecture which utilizes the TVWS spectrum for providing wireless broadband from a HAP. The simulation carried out assumed a coverage area size of 100 km, a 10.5 km cell radius and 121 cells. Results indicated that each cell could provide speeds of up to 27Mbps and 40Mbps when utilizing 64QAM and 256QAM modulation schemes respectively. Finally, the analysis concluded that by leveraging TVWS spectrum from a HAP, there is a potential to carry 5G services to rural customers, even if it does not entirely addresses the KPIs of the 5G network. Among the numerous positive features of HAPs described above, there are some technical challenges that are still to be resolved. Radio coverage extension, capacity enhancement, sidelobe level reduction and antenna used to form the ground cells are very crucial among these issues as they define the performance of the communication system. Spot-beam antennas and array processing methods have been proposed as a solution in [29]–[31]. This paper extends our previous work presented in [4] by analyzing the impact of uniform rectangular HAP antenna arrays (URA) on coverage, capacity and power profile function of exploiting TVWS from HAP. Delivering a TVWS broadband wireless network from a HAP using URA, is a novel idea and to the best of our knowledge this is the first study to present this work. The aim is to reduce the sidelobe levels in the radiation pattern of URA arrays in order to increase the capacity of HAPs networks since they interact with the other cochannel cells. To achieve this, we have developed an array feeding function that can be adjusted to reduce the sidelobe levels using tapering techniques such as Blackman Harris amplitude weighting towards the other cochannel cells in URA, in order to improve the Carrier-to Interference Ratio (CIR). The main contribution of this work can be summarized as follows:

- We examine and promote a type of HAP utilizing TVWS bands as a feasible alternative to provide rural users with broadband networks using a steerable beam URA.
- We present the usage of tapering techniques for reducing sidelobe levels so as to enhance the performance of the proposed system.
- We evaluate the power profile function within a cell which is a function of the antenna array radiation pattern and the slant distance between the HAP and a user.

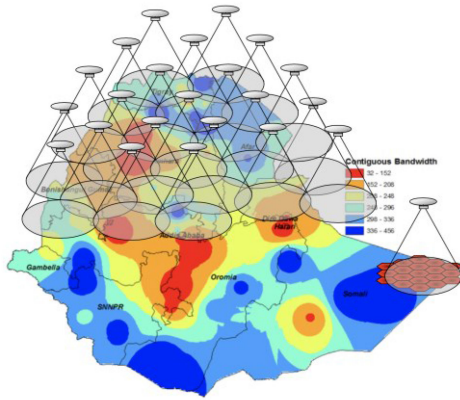


FIGURE 1. A fleet of HAPs demonstrating the future network architecture of HAPs in the Sky in Ethiopia.

- We evaluate the performance of the proposed system in terms CIR contour and coverage probability and truncated Shannon capacity before and after performing tapering technique.
- Power distribution inside a HAP cell is mainly addressed and the key parameters are defined when uniform rectangular antenna arrays is applied in the proposed scenario.

II. TVWS SPECTRUM INVESTIGATION AND HAP NETWORK TOPOLOGY

As a case study, the amount of free TVWS spectrum has been well investigated in [4]–[7] and [32]. In this article, the TVWS spectrums in Ethiopia is taken as an example for our simulation. As per [4] and [5], there are abundant free TVWS spectrum bands in Ethiopia, which can be exploited from a HAP as depicted in Fig. 1. The colored map in Fig. 1 represents the general bandwidth of the contiguous free TVWS in Ethiopia. Using such free TVWS spectrum, there is a possibility to provide wireless connectivity from a HAP. The advantageous position of the HAP in the sky can provide all of the satellite and terrestrial characteristics without their drawbacks. In proposing wireless networks utilizing HAPs, different factors have been addressed, including population density and region size. The overall population of Ethiopia as per [4] is 110000000 and the country’s geographical area is approximately 1104,000 km², while the population density differs greatly from region to region. The footprint area of the HAP depends on the user’s density. The larger the user density, the smaller the footprint will be and the higher the capacity will be accomplished. The diameter of the HAP footprint d for the altitude h of a given base station can therefore be calculated using equation (1) below [33].

$$d = 2 * R \left(\cos^{-1} \left(\frac{R}{R+h} * \cos(\theta) \right) - \theta \right) \quad (1)$$

Where R is the radius of the earth at 6378 km, h is the HAP height, and θ is the minimum elevation angle from the location of the receiver.

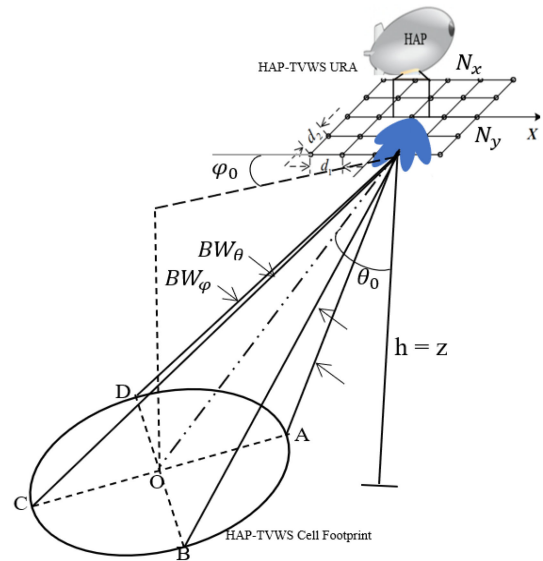


FIGURE 2. URA System with Cell Footprint: HAP cells developed at an altitude of h km from the ground utilizing TVWS.

At an elevation angle of 11.31° and altitude of 20 km above the ground, a HAP provides a diameter of 224.99 km footprint.

Due to the circular nature of the footprint, a single HAP can cover an area of 39,757 km². Thus, Ethiopia will need approximately 28 HAPs to achieve maximum coverage across the country. Fig. 1 illustrates a heat map of the total contiguous bandwidth of the TVWS channel in Ethiopia that can be exploited from the HAP [4]–[7] and [32].

III. SYSTEM MODEL OF HAP EXPLOITING TVWS SPECTRUM

A scenario where a HAP operates in the TVWS band offering downlink communications at an altitude of 20 km by employing directional antennas is considered in this article. The scenario considers a 100 km coverage radius and each cell is a regular hexagon of radius 10.5 km. For beamforming and deploying HAP beams, a payload of 121 TVWS base stations is considered, fitted with a 25 × 25 element URA antenna as depicted in Fig. 2. The phased array antennas are used to build receiver network cells by employing directional beams at about 20 km above the ground from a HAP. To obtain a smooth antenna gain pattern without grating lobes, a maximum $\lambda/2$ spacing between the antenna elements is considered in our phased array architecture [34].

The footprint of a beam has a pointing direction of (θ_0, φ_0) a cross-section half-power beamwidth (HPBW) of BW_θ, BW_φ , and an estimated ellipse-shaped beam projection on the ground for every user on the ground, as seen in Fig. 2. The values of BW_θ and BW_φ are given by [35].

For a URA of $M = N = 25$, $dx = dy = 0.5\lambda$, and scan in the main lobe direction of θ_0 , BW_θ and BW_φ can be defined

as:

$$BW_0 = \text{Sec}(\theta_0 \theta_{x0}) \quad (2)$$

$$BW_\theta = \theta_{x0} \quad (3)$$

Where, $\theta_{x0} = \theta_{y0} = \sin^{-1} \left(\sin \theta_0 + \frac{0.886}{N} \right) - \sin^{-1} \left(\sin \theta_0 - \frac{0.886}{M} \right)$, θ_{x0} and θ_{y0} are the beamwidths of arrays of number of elements equal to M and N respectively.

Due to its simplicity and ease of realistic application, a URA is adopted for this scenario [34]. A URA array factor can be interpreted as a series multiplication of the two linear arrays along the X and Y coordinates. Suppose there are k elements along the X coordinate, then it is possible to describe the Array factor (AF) as:

$$AF_x(\theta, \varphi) = \sum_{k=0}^{K-1} A_x(k) e^{j \frac{2\pi}{\lambda} k d_x \sin \theta \cos \varphi + k\alpha} \quad (4)$$

Where, $\alpha = -\frac{2\pi}{\lambda} d_x \sin \theta_0 \cos \varphi_0$. The complementary angles of elevation and azimuth (θ_0 and φ_0) determine the steering direction for a given beam. Likewise, an array factor along the Y coordinate can be obtained. Consider the Y coordinate has L elements, so it is possible to describe the array factor as:

$$AF_y(\theta, \varphi) = \sum_{l=0}^{L-1} B_y(l) e^{j \frac{2\pi}{\lambda} l d_y \sin \theta \cos \varphi + l\beta} \quad (5)$$

Where $\beta = -\frac{2\pi}{\lambda} d_y \sin \theta_0 \cos \varphi_0$. Thus, the overall array factor is the multiplication of $AF_x(\theta, \varphi)$ and $AF_y(\theta, \varphi)$,

$$\begin{aligned} AF(\theta, \varphi) &= AF_x(\theta, \varphi) AF_y(\theta, \varphi) \\ &= \sum_{k=0}^{K-1} A_x(k) e^{j \frac{2\pi}{\lambda} k d_x \sin \theta \sin \varphi + k\alpha} \\ &\quad \times \sum_{l=0}^{L-1} B_y(l) e^{j \frac{2\pi}{\lambda} l d_y \sin \theta \cos \varphi + l\beta} \end{aligned} \quad (6)$$

$$\begin{aligned} AF(\theta, \varphi) &= \sum_{k=0}^{K-1} \sum_{l=0}^{L-1} A_x(k) e^{j \frac{2\pi}{\lambda} k d_x \sin \theta \sin \varphi + k\alpha} \\ &\quad \times B_y(l) e^{j \frac{2\pi}{\lambda} l d_y \sin \theta \cos \varphi + l\beta} \end{aligned} \quad (7)$$

The 3D array component can often be viewed more conveniently in the X-Y distance coordinates rather than in the θ and φ coordinates [37]. Therefore, θ and φ can be represented as follows:

$$F(X, Y) = |AF(\theta, \varphi)| \quad (8)$$

Where $\theta = \tan^{-1} \left(\frac{Y}{X} \right)$, $\theta = \tan^{-1} \left(\frac{\sqrt{X^2 + Y^2}}{h} \right)$ and h is the HAP altitude to the ground.

As a function of the elevation angle, the gain from a single antenna unit is $G(\theta) = \frac{4\pi d_x d_y}{\lambda^2} \eta \cos \theta$. Where, η is the efficiency of the antenna. Hence, the overall antenna gain can be represented as is the product of the single element gain $G(\theta)$ and

the array factor $AF(\theta, \varphi)$. Thus,

$$G(\theta, \varphi) = G(\theta) AF(\theta, \varphi) \quad (9)$$

A. WINDOW BEAMFORMING FOR URA

A window function is also called the tapering function or weighting function, which is the mathematical function that exists inside the defined interval and does not occur outside of the defined interval. To minimize the sidelobe levels in the antenna array synthesis, window functions can be used [36]–[38].

Hann Window: The weights of the N-point Hanning Window are stated as:

$$w(n) = 0.5 \left(1 - \cos \left(2\pi \frac{n}{N-1} \right) \right); 0 \leq n \leq N-1 \quad (10)$$

Hamming Window: The weights of the N-point Hamming Window are stated as:

$$w(n) = 0.54 - 0.46 \cos \left(2\pi \frac{n}{N-1} \right); 0 \leq n \leq N-1 \quad (11)$$

Blackman-Harris Window: The weights of the N-point Blackman-Harris Window are stated as:

$$\begin{aligned} w(n) &= \alpha_0 + \alpha_1 \cos \left(\frac{2\pi n}{N-1} \right) + \alpha_2 \cos \left(\frac{4\pi n}{N-1} \right) \\ &\quad - \alpha_2 \cos \left(\frac{6\pi n}{N-1} \right); 0 \leq n \leq N-1 \end{aligned} \quad (12)$$

where, $\alpha_0 = 0.35875$, $\alpha_1 = 0.48829$, $\alpha_2 = 0.14128$ and $\alpha_3 = 0.01168$.

B. POWER PROFILE WITHIN A CELL USING URA

As illustrated in Fig. 2, the quantity of energy received by a receiver station within a HAP cell depends on a variety of parameters, including shadowing from surrounding buildings, the array's radiation pattern inside the cell border, and the slant distance between the platform and the receiver. Taking advantage of the altitudes of the HAP in the sky, a free space propagation model is assumed for our received power and power profile function calculations. The majority of produced HAP cells get the most power at their center, and the power declines as the receiver rolls away from the center toward the cell edge. Considering the scenario proposed in Fig. 2 and assuming free-space propagation model between the HAP and the users, the received power, $P_r(\theta_0, \varphi_0)$ is deduced as [39], [40].

$$P_r(\theta_0, \varphi_0) = P_t G_t(\theta_0, \varphi_0) G_r(\theta_0, \varphi_0) \left(\frac{\lambda}{4\pi d(\theta_0)} \right)^2 \quad (13)$$

Where, P_t , $G_t(\theta_0, \varphi_0)$, $G_r(\theta_0, \varphi_0)$ and $d(\theta_0)$, are the transmit power of the HAP cell, antenna gain for HAP, antenna gain of receiver terminal and slant distance between the HAP and the receiver terminal respectively. $G_t(\theta_0, \varphi_0) =$

$|AF(\theta_0, \varphi_0)|^2$ and $d(\theta_0) = \frac{h}{\cos\theta_0} = h \sec\theta_0$. Hence, it is necessary to rewrite the received power as:

$$P_r(\theta_0, \varphi_0) = P_t G_r(\theta_0, \varphi_0) \left(\frac{\lambda}{4\pi h} \right)^2 |AF(\theta_0, \varphi_0)|^2 \cos^2(\theta_0) \quad (14)$$

According to equation (14), the power generated is proportional to the array factor and the receiver's location relative to the HAP station, with other variables being constant. The cell footprint is dependent on both the power gain of the transmission array and the position of the users inside the cell. The square cosine portion is ascribed in this computation to the varying spectrum inside the cell from the HAP to the receiving station, which would vary the power gained in exchange. Hence, it is necessary to rewrite the received power in (14) as:

$$P_r(\theta_0, \varphi_0) = P_t G_r(\theta_0, \varphi_0) \left(\frac{\lambda}{4\pi h} \right)^2 \rho(\theta_0, \varphi_0) \quad (15)$$

Where, $\rho(\theta_0, \varphi_0) = |AF(\theta_0, \varphi_0)|^2 \cos^2(\theta_0)$ is named the power gain profile function, regardless of the array factor and the receiver position, it reflects the difference in the power level obtained. $\rho(\theta_0, \varphi_0)$ represents the fluctuation in the received signal strength caused by the array's gain and the receiver station's location relative to HAP during the receiver station's movement inside the cell. Additionally, it is dependent on the direction of the coverage beam and the receiver station's location relative to the HAP station.

C. CIR, COVERAGE AND CAPACITY PERFORMANCE USING URA

The CIR and coverage probability are assumed to be the most critical radio coverage parameters since they indicate the reuse pattern. This has an influence on the capacity of the system and, as a consequence, on the system's performance. To begin, we will model the proposed system shown in Fig. 3, which has 19 cells, then apply an array feed of URA of 25×25 elements at a HAP of 20 km. According to [41], the $CIR(x, y)$ at each ground point (co-channel cell group) can be determined. We therefore consider a wireless network of transmitters with positions located at $(X_1, Y_1), \dots, (X_n, Y_n)$ in a certain region of space to define the CIR. At a certain location (x, y) , $P_{max}(x, y)$ denotes the maximum received power of a signal at (x, y) from transmitter (X_i, Y_i) and $\sum_{j=1}^n P_i(x, y)$ represents the aggregate interference, which is the total of all other powers. Then, at location (x, y) , the CIR with respect to transmitter (X_i, Y_i) can be obtained as:

$$CIR((x, y), (X_i, Y_i)) = \frac{P_{max}(x, y)}{\sum_{j=1}^n P_i(x, y) - P_{max}(x, y)} \quad (16)$$

The numerator represents the signal and the denominator the interference.

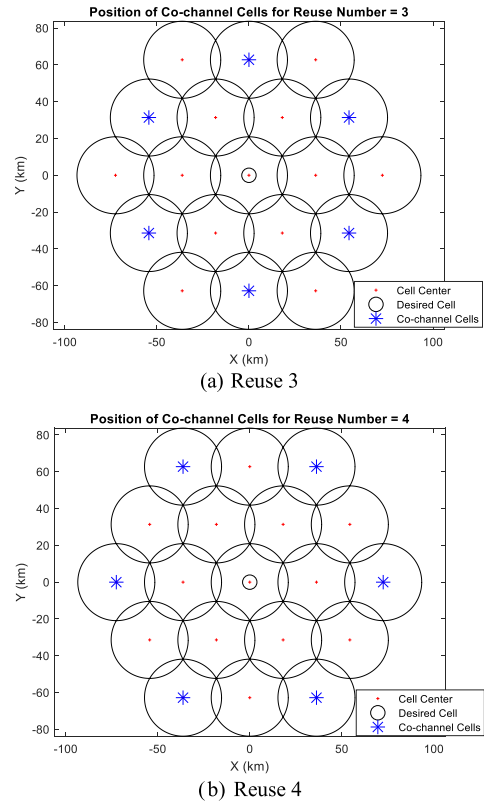


FIGURE 3. Location of Co-channel Cells for (a) Reuse 3 and (b) Reuse 4.

Assuming the CIR at the worst case scenario, the it can be expressed [41] as:

$$P[CIR((x, y), (X_i, Y_i)) > \tau] = \frac{P_{max}(x, y)}{\sum_{j=1}^n P_i(x, y) - P_{max}(x, y)} \quad (17)$$

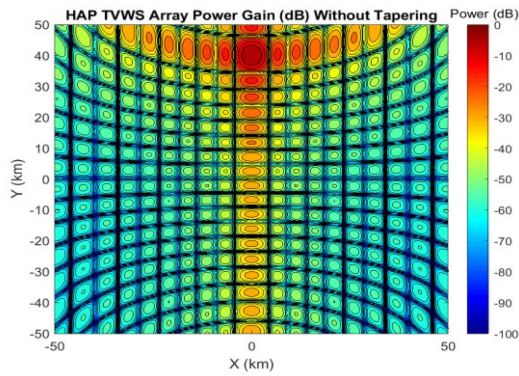
Where, $\tau > 0$ is the CIR threshold. For the value stated τ , the probability $P[CIR((x, y), (X_i, Y_i)) > \tau]$ is called the coverage probability, which is simply the probability that a signal coming from (X_i, Y_i) can be received successfully at location (x, y) . The capacity performance of the proposed system can be obtained from the Carrier to Interference plus Noise Ratio (CINR).

$$CINR = \frac{P_R(x, y)}{\sum_{j=1}^n P_i(x, y) + P_N} \quad (18)$$

Where, $P_R(x, y)$ is the received power level of the user at location (x, y) , P_n is the noise power and $\sum_{j=1}^n P_i(x, y)$ is the number of the neighboring cells' interfering power. In a wireless communication network, the level of CINR may be used to assess channel capacity. The system or user equipment may employ only a certain CINR (which results in 64-QAM and 256-QAM modulation schemes), and as a consequence, every link in the system is supported by a maximum of CINR values. If the physical data rate for the i^{th} user in a link is C_i the Shannon-Hartley theorem gives an upper limit on the channel's capacity as $C_i = B_i \log_2(1 + CINR_i)$, where B_i is the bandwidth of the i^{th} link. The truncated Shannon bound

TABLE 1. Parameters for Simulation

Parameter	Value
Minimum Elevation angle (Degree)	11.31
Bandwidth (MHz)	8
Carrier Frequency (MHz)	617
Reuse Number	4
Temperature (K)	500
Number of Cells	121
HAP Antenna Gain (dB)	20
Transmit Power (dBW)	10
Boltzmann's Constant (J/K)	1.3807×10^{-23}
Thermal Noise Power (dB)	-132.5806
Array Size	25x25
Element Spacing along X and Y	$\lambda/2$


FIGURE 4. Contour of HAP TVWS Array factor (HAP TVWS Array Power Gain) of an 25x25 URA steered at (040) km before applying tapering techniques.

[42] is a representation of the channel's practical achievable capacity and is described in equation 19 as:

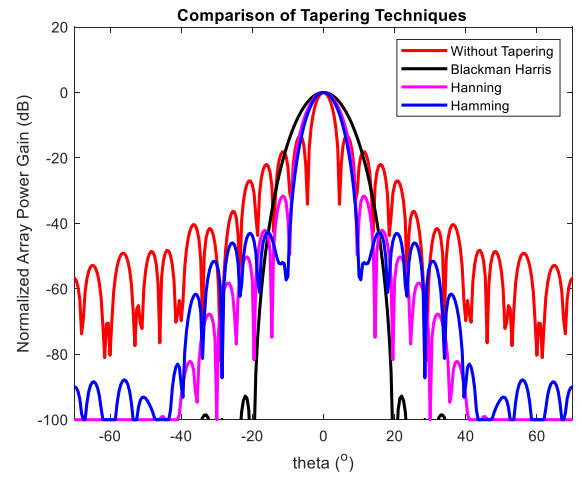
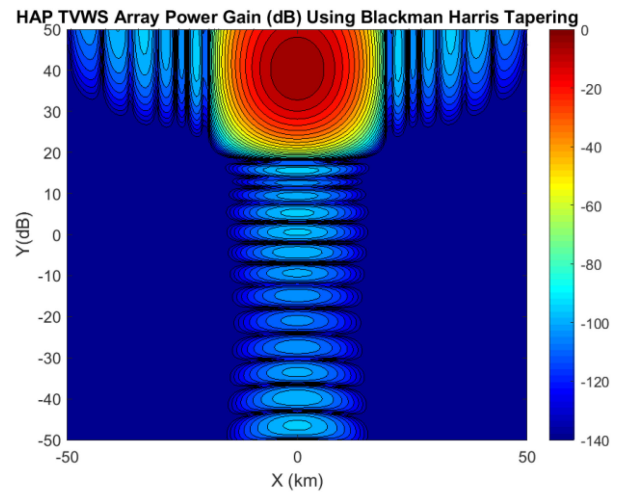
$$C_i = \begin{cases} 0, & CINR_i (dB) < CINR_{min} \\ \alpha B_i \log_2 (1 + CINR_i), & CINR_{min} \leq CINR_i \leq CINR_{max} \\ C_{max}, & CINR_i (dB) > CINR_{max} \end{cases} \quad (19)$$

Where, α is an attenuation factor that represents the link's implementation loss and is set to 0.65, $CINR_{min} = 1.8 \text{ dB}$ and $CINR_{max} = 30 \text{ dB}$ and $CINR_i \in (CINR_{min}, CINR_{max})$.

IV. RESULTS AND DISCUSSIONS

The proposed scenario's simulation results are based on the simulation parameters listed in Table 1.

The array factor of a 25×25 rectangular array steering at the ground position (0, 40) km is depicted in 2D contour plot in Fig. 4. Dark red denotes the maximum power (or main lobe). As it can be seen from the diagram, sidelobe levels have a high value, which would impact the quality of the main beam and cause unnecessary interference. Hence, the Blackman Harris tapering technique has been proposed to lower such sidelobe levels and results have been promising, as illustrated in Fig. 6.


FIGURE 5. Comparison of Tapering Techniques.

FIGURE 6. Optimized contour of HAP TVWS Array factor (Power Gain) of an 25×25 URA steered at (040)km after applying Blackman Harris tapering technique.

Beampattern optimization necessitates the design of antenna element weights. Fig. 5 shows that the Blackman Harris window outperforms the other techniques such as Hanning, Hamming, and without tapering, where lower sidelobe levels can be achieved at the expense of a wider beamwidth. The amount of sidelobes is therefore significantly reduced. However, when Blackman Harris weights are applied, the 3 dB beamwidth becomes wider than other amplitude weights. As it can be seen in Fig. 6, Blackman Harris tapering is the best tapering technique so as to avoid the sidelobe level that occurs around the desired area, and this in turn improves the CIR performance.

The antenna beamwidth is another key component that impacts system performance. It governs the directionality of the antenna and, as a consequence, the footprint on the ground, as depicted in Fig. 7. As shown, a narrow beamwidth may result in a high peak gain and a quick decline in antenna gain as the angle extended from the boresight rises. At the edge of

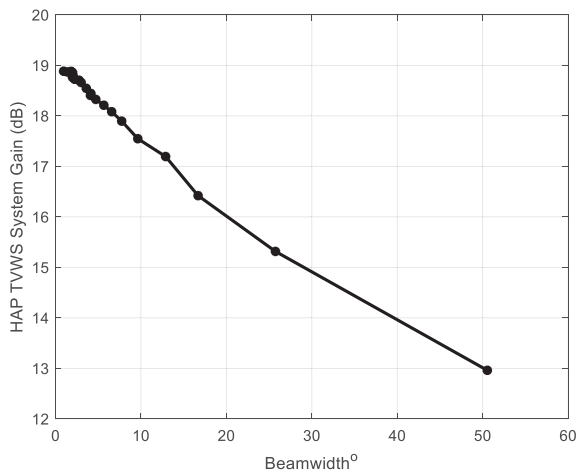


FIGURE 7. Antenna gain as a function of beamwidth.

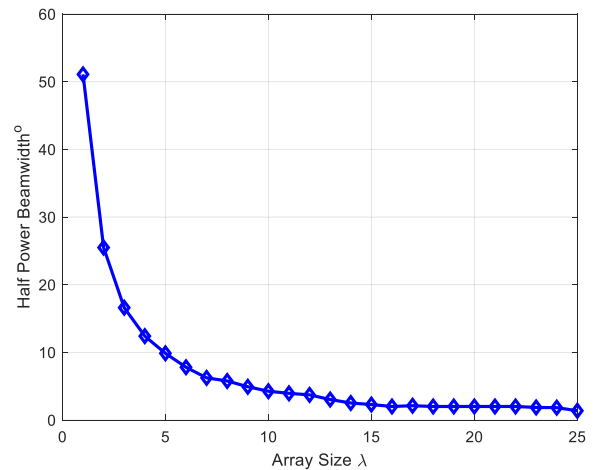


FIGURE 9. Beamwidth versus number of arrays.

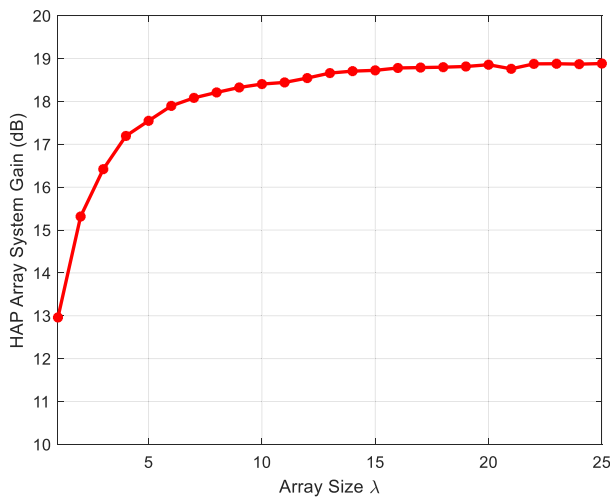


FIGURE 8. HAP Array Power Gain versus Arrays Size.

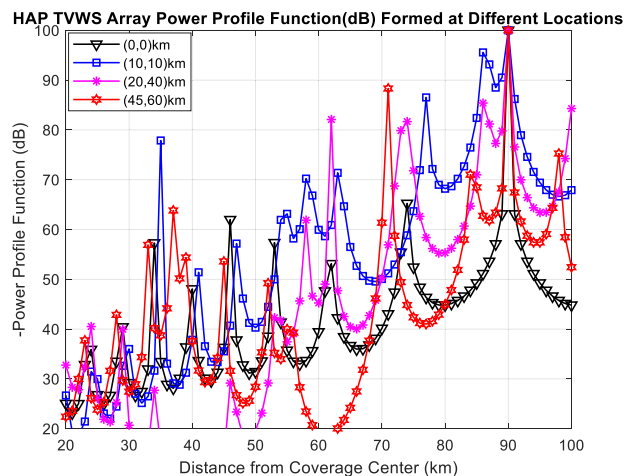


FIGURE 10. Power profile function.

the HAP coverage region, the antenna gain attenuates to the required level to keep the effect of co-channel interferences to a manageable level [39], [40].

As illustrated in Fig. 8, it can be noted that by increasing the number of elements of the antenna array, the performance gradually improves. Fig. 9, shows how the beamwidth changes as the number of arrays increases. If the number of elements in the array grows, the beamwidth decreases. Thus, making the antenna more directional so as to point to the desired location.

There are a variety of parameters that impact the receive power of a receiver station in a HAP cell. These factors include the radiation pattern of the antenna array used to create the coverage cells, the elevation angle of the receiver from the platform, as well as the slant distance from the platform to the receiver. All must be considered when determining the received power. As a result, the attenuation of the signal at a given frequency is determined by the power profile function. Fig. 10 shows the power profile feature in decibels for a 20 x

20 element array with a platform altitude of 20 kilometers. As it can be seen from Fig. 11, as we move away from the center of the cell, CIR values become smaller and smaller. Moreover, the power profile function value at different locations is presented by steering the angles to the desired location such as at (0, 0), (10, 10), (20, 40) and (45, 60)km.

The CIR and coverage performance of the HAP wireless system using TVWS spectrum is presented in Fig. 11, where 19 cells provide coverage with a reuse factor of 4. Fig. 11 illustrates how the CIR changes with distance in the covered region. While calculating CIR variance with and without utilizing tapering strategies, Fig. 11 depicts the CIR contour at a cluster size of four. The URA CIR variation is shown as a function of distance in Fig. 11. With a maximum of 22 dB at the cell centers and a minimum of 2 dB at the cell margins, the CIR varies from 2 to 22 dB as the distance from the center of the cell increases. The low CIR values are due to the high sidelobe levels of the URA. It is noticed that after applying the tapering technique, the CIR value has improved to 30 dB and 5 dB at the cell center and cell edge respectively. The CIR

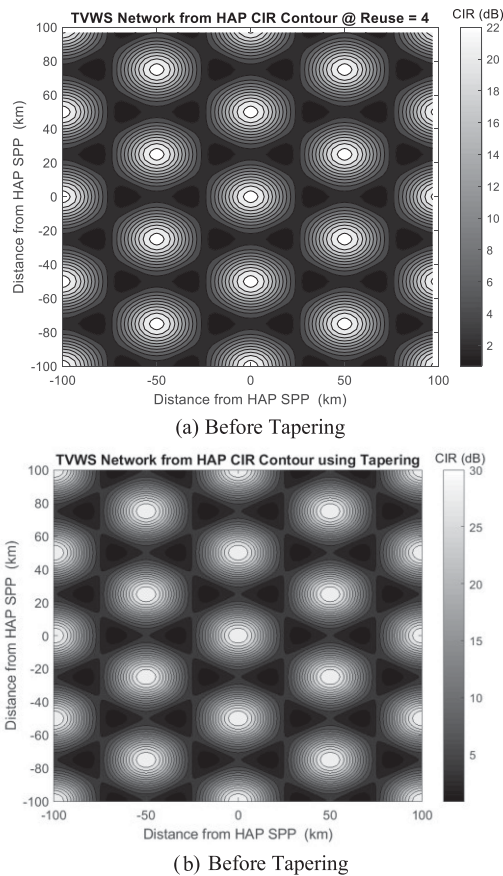


FIGURE 11. CIR Contour of Reuse 4 (a) before tapering and (b) after tapering.

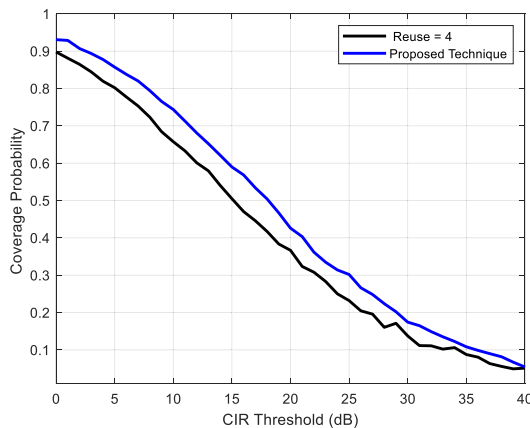


FIGURE 12. Coverage performance for reuse of 4 and proposed technique.

value has improved by 8 dB at cell center and by 3 dB at the cell edge which shows the tapering technique has improved the performance of the communication system by reducing the sidelobe levels.

To represent the distribution of the CIR within the cells, Fig. 12 illustrates the fractional area that may be covered by at least a specific CIR degree. The increase in CIR achieved by the proposed beamforming technique over the other traditional schemes, which seem to be quite close together, is

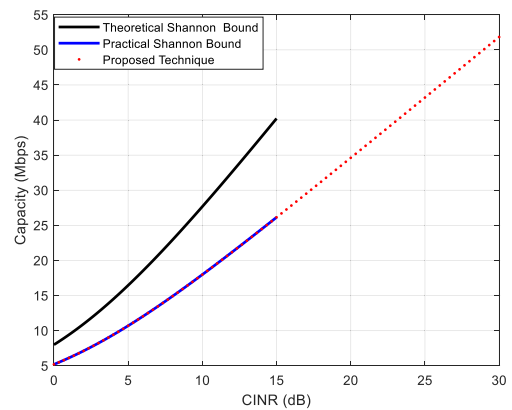


FIGURE 13. TVWS based HAP Channel Capacity a function of CINR.

clearly visible in this figure. It is possible to display the distribution of the CIR inside the cells via fractional coverage as seen in Fig. 12. It indicates the fractional region which can be filled by at least a particular level of CIR. The figure shows the coverage performance plots utilizing 25×25 URA for frequency reuse 4 with and without applying tapering technique as a function of CIR threshold values. Based on this illustration, it is obvious that higher CIR coverage was achieved by adopting the suggested beamforming methodology.

Fig. 13 illustrates the theoretical Shannon bound channel capacity and truncated practical Shannon capacity as a function of CINR for reuse of 4 before and after applying tapering. After applying, the proposed model on practical Shannon bound scheme, the capacity increases with the CINR values. As can be seen from the figure, the practical upper bound channel capacity after applying the proposed technique is about 53 Mbps which is greater than the theoretical value and the practical Shannon bound value without tapering. Therefore, Fig. 13 demonstrated that the proposed model outperforms the theoretical and practical Shannon bound schemes.

V. CONCLUSION

In sparsely inhabited environments, the introduction of traditional communication networks by telecom operators is not economically feasible. Researchers around the world are investigating the prospect of utilizing the underused/unused part of the TV spectrum (specially the UHF band) as a low-cost solution to wireless broadband network. The deployment of TVWS networks from High Altitude Platforms (HAPs) using UHF bands is an effective way of delivering wireless broadband connectivity to such areas. We believe that the use of HAP-based networks could be a feasible alternative to provide rural users with broadband networks using a steerable beam uniform rectangular array (URA). Coverage, capacity and power profile analysis has been presented in this paper. The channel capacity for the theoretical Shannon bound and practical truncated Shannon bound are determined and compared. As per the simulation our proposed system is the best candidate for rural scenario with the upper bound practical capacity of 53Mbps.

REFERENCES

- [1] CISCO, Annual Internet Report (2018–2023) White paper, Accessed: Jan. 2022. [Online]. Available: <https://www.cisco.com/c/en/us/solutions/collateral/execperspectives/annual-internet-report/white-paper-c11-741490.html>
- [2] I. T. U., “ITU releases 2018 global and regional ICT estimates union, international telecommunication,” 2018. Accessed: Jan. 2021. [Online]. Available: <https://www.itu.int>
- [3] I. T. U., International Telecommunications Union, “ICT facts and figures 2017,” *Itu*, 2017. Accessed: Jan. 2021. [Online]. Available: www.itu.int/ict
- [4] K. Katzis, L. Mfupe, and H. M. Hussien, “Opportunities and challenges of bridging the digital divide using 5G enabled high altitude platforms and TVWS spectrum,” in *Proc. IEEE 8th Int. Conf. Commun. Netw.*, 2020, pp. 1–7, doi: [10.1109/ComNet47917.2020.9306090](https://doi.org/10.1109/ComNet47917.2020.9306090).
- [5] H. Mohammed, K. Katzis, L. Mfupe, and E. T. Bekele, “Practical implementation of geo-location TVWS database for Ethiopia,” in *Proc. Int. Conf. Adv. Sci. Technol.*, 2020, pp. 495–510, doi: [10.1007/978-3-030-80618-7_34](https://doi.org/10.1007/978-3-030-80618-7_34).
- [6] H. M. Hussien, K. Katzis, L. P. Mfupe, and E. T. Bekele, “Coexistence of TV white space devices and DTV services in ethiopian geolocation white space spectrum database,” in *Proc. IEEE 24th Int. Workshop Comput. Aided Model. Des. Commun. Links Netw.*, 2019, pp. 1–5, doi: [10.1109/CAMAD.2019.8858472](https://doi.org/10.1109/CAMAD.2019.8858472).
- [7] T. T. Terefe, H. M. Hussien, and S. F. Meko, “Reserved distance and significant parameter determination in incumbent and TV white space system coexistence,” in *Proc. Int. Conf. Adv. Sci. Technol.*, 2021, pp. 125–133, doi: [10.1007/978-3-030-80621-7_9](https://doi.org/10.1007/978-3-030-80621-7_9).
- [8] J. Thornton, D. Grace, C. Spillard, T. Konefal, and T. C. Tozer, “Broadband communications from a high-altitude platform: The European helinet programme,” *Electron. Commun. Eng. J.*, vol. 13, no. 3, pp. 138–144, 2001, doi: [10.1049/ecej:20010304](https://doi.org/10.1049/ecej:20010304).
- [9] S. Karapantazis and F. N. Pavlidou, “The role of high altitude platforms in beyond 3G networks,” *IEEE Wireless Commun.*, vol. 12, no. 6, pp. 33–41, Dec. 2005, doi: [10.1109/MWC.2005.1561943](https://doi.org/10.1109/MWC.2005.1561943).
- [10] D. Grace, N. E. Daly, T. C. Tozer, A. G. Burr, and D. A. J. Pearce, “Providing multimedia communications services from high altitude platforms,” *Int. J. Satell. Commun.*, vol. 19, no. 6, pp. 559–580, 2001, doi: [10.1002/sat.698](https://doi.org/10.1002/sat.698).
- [11] S. C. Arum *et al.*, “A review of wireless communication using high-altitude platforms for extended coverage and capacity,” *Comput. Commun.*, vol. 157, pp. 232–256, 2020, doi: [10.1016/j.comcom.2020.04.020](https://doi.org/10.1016/j.comcom.2020.04.020).
- [12] H. M. Hussien *et al.*, “Bridging the urban-rural broadband connectivity gap using 5G enabled HAPs communication exploiting TVWS spectrum,” *J. Eng. Res. Sci.*, vol. 1, no. 1, pp. 24–32, 2022, doi: [10.55708/jso102003](https://doi.org/10.55708/jso102003).
- [13] S. Karapantazis and F. Pavlidou, “Broadband communications via high-altitude platforms: A survey,” *IEEE Commun. Surv. Tuts.*, vol. 7, no. 1, pp. 2–31, Jan.–Mar. 2005, doi: [10.1109/COMST.2005.1423332](https://doi.org/10.1109/COMST.2005.1423332).
- [14] C. L. Spillard, D. Grace, J. Thornton, and T. C. Tozer, “Effect of ground station antenna beamwidth on rain scatter interference in high-altitude platform links,” *Electron. Lett.*, vol. 38, no. 20, pp. 1211–1213, Sep. 2002, doi: [10.1049/el:20020823](https://doi.org/10.1049/el:20020823).
- [15] I.T.U., International Telecommunication Union, *Report of the CPM On Technical, Operational and Regulatory/Procedural Matters to Be Considered by the World Radiocommunication Conference 2019*, Sharm El-Sheikh, Egypt: ITU Publications, 2019.
- [16] F. Dovis, R. Fantini, M. Mondin, P. Savi, D. Elettronica, and P. Torino, “4G Communications based on high altitude stratospheric platforms: Channel modeling and performance evaluation,” in *Proc. IEEE Glob. Telecommun. Conf.*, 2001, pp. 557–561, doi: [10.1109/GLOCOM.2001.965179](https://doi.org/10.1109/GLOCOM.2001.965179).
- [17] I.T.U., “Minimum performance characteristics and operational conditions for high altitude platform stations providing IMT-2000 in the bands 1885–1980 MHz, 2010–2025 MHz and 2110–2170 in the regions 1 and 3 and 1885–1980 MHz and 2110–2170 MHz in region 2. - Recommendation,” I.T.U., Geneva, Switzerland, Tech. Rep. ITU-R M.1456, 2000.
- [18] Y. C. Foo, W. L. Lim, R. Tafazolli and L. W. Barclay, “Forward link power control for high altitude platform station W-CDMA system,” in *Proc. IEEE 54th Veh. Technol. Conf. VTC Fall 2001. Proc. (Cat. No.01CH37211)*, vol. 2, 2001, pp. 625–629, doi: [10.1109/VTC.2001.956845](https://doi.org/10.1109/VTC.2001.956845).
- [19] Z. Yang, A. Mohammed, T. Hult, and D. Grace, “Downlink coexistence performance assessment and techniques for WiMAX services from high altitude platform and terrestrial deployments,” *EURASIP J. Wireless Commun. Netw.*, vol. 2008, 2008, Art. no. 291450, doi: [10.1155/2008/291450](https://doi.org/10.1155/2008/291450).
- [20] G. Arantit *et al.*, “Hybrid system HAP-Wi-Fi for incident area network,” in *Proc. Int. Conf. Pers. Satell. Serv.*, vol. 43, 2010, pp. 436–445, doi: [10.1007/978-3-642-13618-4_33](https://doi.org/10.1007/978-3-642-13618-4_33).
- [21] S. Bayhan, K. Gür, and F. Alagöz, “High altitude platform (HAP) driven smart radios: A novel concept,” in *Proc. Int. Workshop Satell. Space Commun.*, 2007, pp. 201–205, doi: [10.1109/IWSSC.2007.4409416](https://doi.org/10.1109/IWSSC.2007.4409416).
- [22] U. A. Shital Joshi, “Energy efficient cognitive radio network using high altitude platform station,” in *Proc. Future Inf. Commun. Conf.*, 2018, pp. 190–202, doi: [10.1007/978-3-030-03402-3_14](https://doi.org/10.1007/978-3-030-03402-3_14).
- [23] S. C. Arum, D. Grace, P. D. Mitchell, and M. D. Zakaria, “Beam-pointing algorithm for contiguous high-altitude platform cell formation for extended coverage,” in *Proc. IEEE 90th Veh. Technol. Conf.*, 2019, pp. 1–5, doi: [10.1109/VTCfall.2019.8891528](https://doi.org/10.1109/VTCfall.2019.8891528).
- [24] Q. Xi, C. He, L. Jiang, J. Tian, and Y. Shen, “Capacity analysis of massive MIMO on high altitude platforms,” in *Proc. IEEE Glob. Commun. Conf.*, 2016, pp. 1–6, doi: [10.1109/GLOCOM.2016.7841647](https://doi.org/10.1109/GLOCOM.2016.7841647).
- [25] G. P. White and Y. V. Zakharov, “Data communications to trains from high-altitude platforms,” *IEEE Trans. Veh. Technol.*, vol. 56, no. 4, pp. 2253–2266, Jul. 2007, doi: [10.1109/TVT.2007.897185](https://doi.org/10.1109/TVT.2007.897185).
- [26] Loon_Project, Accessed: Jan. 2022. [Online]. Available: <https://loon.com/technology/>
- [27] S. Ananth, B. Wojtowicz, A. Cohen, N. Gulia, A. Bhattacharya, and B. Fox, “System design of the physical layer for Loon’s high-altitude platform,” *EURASIP J. Wireless Commun. Netw.*, vol. 2019, Art. no. 170, 2019, doi: [10.1186/s13638-019-1461-x](https://doi.org/10.1186/s13638-019-1461-x).
- [28] J. Lun *et al.*, *Solar Powered High Altitude Platform and Terrestrial Infrastructures*. York, U.K.: Univ. York, 2017.
- [29] S. Karapantazis and F. Pavlidou, “Broadband communications via high-altitude platforms: A survey,” *IEEE Commun. Surv. Tut.*, vol. 7, no. 1, pp. 2–31, Jan.–Mar. 2005, doi: [10.1109/COMST.2005.1423332](https://doi.org/10.1109/COMST.2005.1423332).
- [30] Z. Yang and A. Mohammed, “Evaluation of WiMAX uplink performance in high altitude platforms cellular system,” in *Proc. 4th Int. Symp. Wireless Commun. Syst.*, 2007, pp. 834–837, doi: [10.1109/ISWCS.2007.4392458](https://doi.org/10.1109/ISWCS.2007.4392458).
- [31] A. Mohammed and T. Hult, “Capacity evaluation of a high altitude platform diversity system equipped with Compact MIMO antennas,” *Int. J. Recent Trends Eng.*, vol. 1, May 2009, Art. no. 3.
- [32] H. M. Hussien, K. Katzis, L. P. Mfupe, and T. Ephrem, “Calculation of TVWS spectrum availability using geo-location white space spectrum database,” in *Proc. IEEE AFRICON*, 2021, pp. 1–6, doi: [10.1109/AFRICON51333.2021.9570915](https://doi.org/10.1109/AFRICON51333.2021.9570915).
- [33] Iskandar and D. R. Putro, “Performance evaluation of broadband WiMAX services over high altitude platforms (HAPs) communication channel,” in *Proc. 4th Int. Conf. Wireless Mobile Commun.*, 2008, pp. 55–59, doi: [10.1109/ICWMC.2008.20](https://doi.org/10.1109/ICWMC.2008.20).
- [34] C. A. Balanis, *Antenna Theory Analysis and Design*. Hoboken, NJ, USA: Wiley, 1982.
- [35] R. S. Elliott, “Beamwidth and directivity of large scanning arrays,” *Microw. J.*, vol. 7, pp. 74–82, 1964.
- [36] F. J. Harris, “On the use of windows for harmonic analysis with the discrete Fourier transform,” *Proc. IEEE*, vol. 66, no. 1, pp. 51–83, Jan. 1978, doi: [10.1109/PROC.1978.10837](https://doi.org/10.1109/PROC.1978.10837).
- [37] Z. Xu, G. White, and Y. Zakharov, “Optimisation of beam pattern of high-altitude platform antenna using conventional beamforming,” *Proc. IEEE*, vol. 153, no. 6, pp. 865–870, Jan. 2007, doi: [10.1049/IP-COM:20050355](https://doi.org/10.1049/IP-COM:20050355).
- [38] A. Nuttall, “Some windows with very good sidelobe behavior,” *IEEE Trans. Acoust., Speech, Signal Process.*, vol. 29, no. 1, pp. 84–91, Feb. 1981, doi: [10.1109/TASSP.1981.1163506](https://doi.org/10.1109/TASSP.1981.1163506).
- [39] K. Katzis, D. A. J. Pearce, and D. Grace, “Fairness in channel allocation in a high altitude platform communication system exploiting cellular overlap,” in *Proc. Wireless Pers. Multimedia Commun. Conf.*, 2004, pp. 232–256.
- [40] K. Katzis, D. A. J. Pearce, and D. Grace, “Fixed channel allocation techniques exploiting cell overlap for high altitude platforms,” *Cell*, vol. 1, no. A2, pp. B1, 2004.
- [41] J. Thornton, D. Grace, M. H. Capstick, and T. C. Tozer, “Optimizing an array of antennas for cellular coverage from a high altitude platform,” *IEEE Trans. Wireless Commun.*, vol. 2, no. 3, pp. 484–492, May 2003, doi: [10.1109/TWC.2003.811052](https://doi.org/10.1109/TWC.2003.811052).

- [42] A. Papadogiannis and A. G. Burr, "Multi-beam assisted MIMO — A novel approach to fixed beamforming," in *Proc. Future Netw. Mobile Summit*, 2011, pp. 1–8.



HABIB MOHAMMED HUSSIEN received the bachelor's degree from Adama Science and Technology University, Adama, Ethiopia, in 2008, and the M.Sc. degree in electrical and electronic engineering (signal and information processing technology) from Tianjin University, Tianjin, China, in 2012. He is currently working toward the Ph.D. degree with the Addis Ababa Institute of Technology, Addis Ababa University, Addis Ababa, Ethiopia. His current research interests include high-altitude platform, handoff schemes, TV white space technology, radio resource allocation and optimization, call admission control, heterogeneous network coexistence issues, and 5G IoT.



KONSTANTINOS KATZIS (Senior Member, IEEE) received the B.Eng. degree in computer systems engineering and the M.Sc. degree in radio systems engineering from the University of Hull, Hull, U.K., in 2000 and 2001, respectively, and the Ph.D. degree in electronics from the University of York, York, U.K. His current research interests include dynamic spectrum access and cognitive radio, architectures for 5G, and beyond and wireless communications from aerial platforms.

He has also been working toward the development of highly efficient resource allocation techniques and handoff techniques optimized for the operation of high-altitude platform communication systems. His work involved modeling of the platform movements and simulating the effects on the communications. He is currently the Secretary in IEEE1900.6 Standard and also MC member of COST action CA20120 (Intelligence-Enabling Radio Communications for Seamless Inclusive Interactions - INTERACT).

Recently, he has been awarded with the Fulbright Visiting Scholar fund for his proposal "Requirement Analysis of 5G Networks Supporting IoT-Health Applications" in collaboration with the Information Technology Laboratory of the National Institute of Standards and Technology in Washington DC (USA). Dr. Konstantinos Katzis is an Associate Professor with European University Cyprus.



LUZANGO PANGANI MFUPE (Senior Member, IEEE) received the bachelor's, master's, and Ph.D. degrees in electrical engineering from the Tshwane University of Technology, Pretoria, South Africa. He is currently an experienced Principal Research Scientist, Innovator, and Entrepreneur with demonstrated leadership in large and cutting-edge technology projects. He has technical skill in dynamic spectrum management, television white spaces, and defense. He is an Experienced Civilian in spectrum sharing models,

formulation of spectrum regulations and policies, development of geo-location spectrum databases, advanced wireless networks design and modeling, satellite communications, airborne wireless networks, artificial intelligence/machine learning for future wireless communications, such as 5G, computer simulations, lecturing, supervision, and SMMEs support.



EPHREM TESHALE BEKELE (Senior Member, IEEE) received the B.Sc. degree in electrical engineering from Bahir Dar University, Bahir Dar, Ethiopia, in 2007, the M.Sc. degree in telecommunications engineering and the Ph.D. degree in information and communications technology from the University of Trento, Trento, Italy, in 2011 and 2015, respectively. From 2007 to 2009, he was an Assistant Lecturer with Bahir Dar University. He is currently an Assistant Professor with the Addis Ababa Institute of Technology (AAiT), Addis

Ababa University, Addis Ababa, Ethiopia, and an Associate Faculty Member of the ELEDIA Research Center. He is also a Visiting Lecturer with Bahir Dar University, and a member of the Applied Electromagnetic Research Group, AAiT. His main research interests include electromagnetic nondestructive testing, technology 'domestication', and RF regulation.